

Structural Simplification of Bioactive Natural Products with Multicomponent Synthesis. 3. Fused Uracil-Containing Heterocycles as Novel Topoisomerase-Targeting Agents

Nikolai M. Evdokimov,[†] Severine Van slambrouck,[†] Petra Heffeter,[†] Lee Tu,[†] Benjamin Le Calvé,[§] Delphine Lamoral-Theys,[§] Carla J. Hooten,[†] Pavel Y. Uglinskii,^{||} Snezna Rogelj,[†] Robert Kiss,[§] Wim F. A. Steelant,[†] Walter Berger,[‡] Jeremy J. Yang,[#] Cristian G. Bologa,[#] Alexander Kornienko,^{*,†} and Igor V. Magedov^{*,†}

[†]Department of Chemistry, New Mexico Institute of Mining and Technology, Socorro, New Mexico 87801, United States

[‡]Institute of Cancer Research, Department of Medicine I, Medical University of Vienna, Borschkegasse 8a, 1090 Vienna, Austria

[§]Laboratoire de Toxicologie and Laboratoire de Chimie Analytique, Toxicologie et Chimie Physique Appliquée, Institut de Pharmacie, Université Libre de Bruxelles, Brussels, Belgium

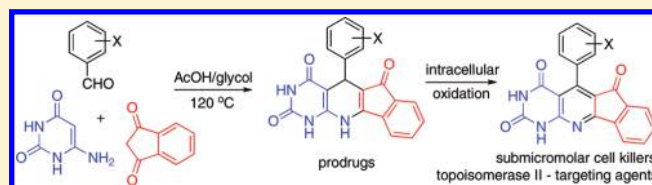
^{||}Department of Organic Chemistry, Timiryazev Agriculture Academy, Moscow 127550, Russia

[†]Department of Biology, New Mexico Institute of Mining and Technology, Socorro, New Mexico 87801, United States

[#]Division of Biocomputing, Department of Biochemistry and Molecular Biology, University of New Mexico School of Medicine, Albuquerque, New Mexico 87131, United States

S Supporting Information

ABSTRACT: After the initial discovery of antiproliferative and apoptosis-inducing properties of a camptothecin-inspired pentacycle based on a 1*H*-indeno[2',1':5,6]dihydropyrido[2,3-*d*]pyrimidine scaffold, a library of its analogues as well as their oxidized planar counterparts were prepared utilizing a practical multicomponent synthetic protocol. The synthesized compounds exhibited submicromolar to low micromolar antiproliferative potencies toward a panel of human cancer cell lines. Biochemical experiments are consistent with the dihydropyridine library members undergoing intracellular oxidation to the corresponding planar pyridines, which then inhibit topoisomerase II activity, leading to inhibition of proliferation and cell death. Because of facile synthetic preparation and promising antitopoisomerase activity, both the dihydropyridine and planar pyridine-based compounds represent a convenient starting point for anticancer drug discovery.



INTRODUCTION

Natural products have traditionally been an excellent source of new medicinal leads, and their role in drug discovery is especially pronounced in the area of cancer pharmacology, where the fraction of the drugs derived from natural products amounts to 60%.¹ Generally, however, research efforts in this area are greatly impeded by the structural complexity of natural products and their poor availability from natural sources. Many laboratories have tackled these problems by preparing libraries of structurally simplified natural product analogues utilizing *de novo* synthetic pathways.² The approach practiced in our laboratory involves the design of natural product or natural product-mimetic scaffolds, which can be synthetically accessed in one-step by utilizing multicomponent reactions (MCR),³ followed by preparation and biological evaluation of compound libraries based on these scaffolds. We have demonstrated that amalgamation of multicomponent chemistry, characterized by synthetic efficiency and diversity, with biorelevance, offered by natural products, facilitates the generation of high quality leads for drug discovery.⁴ For example, we showed that the

stereochemically complex structure of an important anticancer lead podophyllotoxin and pyranoquinolone alkaloids can be efficiently simplified with mimetic scaffolds that retain antitubulin activity of the natural products and are accessible via one-step MCRs.⁴

In continuation of these efforts, we have been investigating multicyclic scaffolds, designed to be mimetics of DNA and topoisomerase-targeting natural products, such as a topoisomerase I poison, camptothecin (**1**, Figure 1). This natural product was isolated from extracts of *Camptotheca acuminata*, a tree extensively used in traditional Chinese medicine.⁵ Due to limited water solubility and high levels of toxicity, the clinical trials aimed at evaluation of camptothecin as an anticancer drug were suspended.⁶ However, the investigation of camptothecin analogues resulted in two clinically useful agents, topotecan (**2**) and irinotecan, employed for the treatment of colon and ovarian cancer, respectively.⁷ Numerous mechanistic studies have revealed that camptothecin and its derivatives have no affinity for

Received: July 26, 2010

Published: March 09, 2011

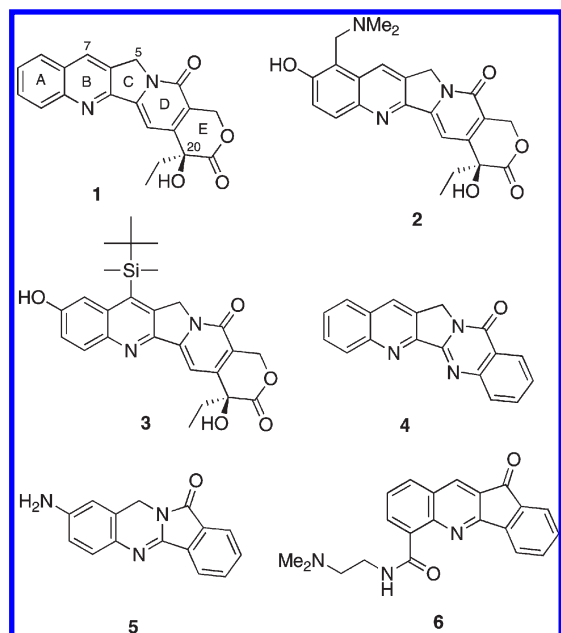


Figure 1. Structures of camptothecin (1), topotecan (2), silatecan (3), luotonin A (4), batracylin (5), and indenopyridine 6.

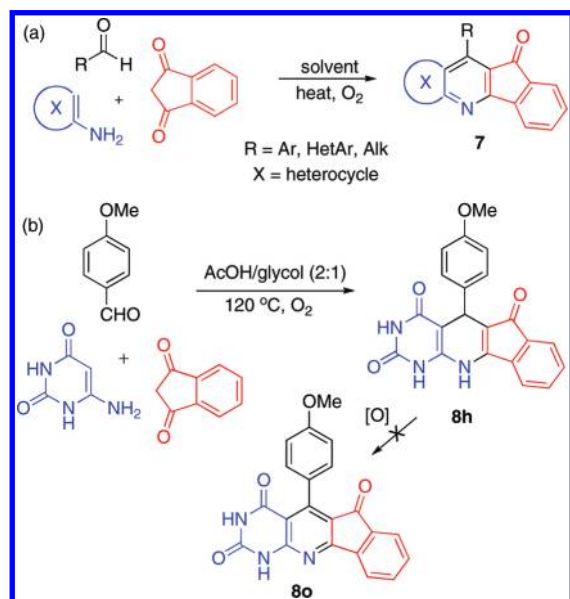


Figure 2. (a) MCR used for the preparation of heterofused indenopyridines 7 and (b) preparation of the uracil-fused pentacycle 8h in the dihydropyridine form.

either DNA or topoisomerase I alone but bind to the topoisomerase I–DNA complex, stabilizing a covalent phosphotyrosyl intermediate and causing single strand DNA breaks.⁸ Aided by the availability of topotecan–topoisomerase I–DNA and camptothecin–topoisomerase I–DNA crystal structures as well as computational docking models, numerous analogues have been prepared, generating extensive SAR data.⁸ These data reveal the absolute requirement for conjugation and planarity of rings A, B, C, and D, important for the full intercalation into the duplex DNA within the covalent topoisomerase I–DNA complex. In addition, large substituents at C-7 are not only well tolerated but also result in analogues with higher levels of cytotoxicity and significantly improved *in vivo* activity.⁹ For

example, a number of so-called silatecans (e.g., 3) have entered clinical trials.¹⁰ The long-standing belief that the E-ring lactone is essential has recently been put into question.¹¹ One important observation in this regard is the potent cytotoxicity and stabilization of the topoisomerase I–DNA binary complex, with the same sequence selectivity as that of camptothecin itself, by luotonin A (4), a naturally occurring congener of camptothecin.¹²

Importantly, several reports have shown that the complex ring system in camptothecin is not critical and similar types of activity could be found in compounds based on indenoquinazoline or indenoquinoline skeletons, respectively present in batracylin (5) and synthetic tetracycle 6. Batracylin is an experimental anticancer drug active as a dual topoisomerase I/II poison and inducer of unscheduled DNA synthesis in nonproliferating cells,¹³ while compound 6 and its closely related analogues are studied for their strong DNA binding properties and dual topoisomerase I/II targeting.¹⁴ Therefore, with the goal of developing potential anticancer agents acting through topoisomerase targeting, we developed a one-step multicomponent condensation of various aminoheterocycles, aldehydes, and 1,3-indanedione, leading to the synthesis of various heterofused indenopyridines 7 (Figure 2a).¹⁵ In addition to offering the possibility to explore a heterocyclic replacement of ring A in these camptothecin-inspired libraries, such an approach allowed for an installation of a C-7 substituent (camptothecin numbering) found to be beneficial for the improved anticancer properties associated with camptothecin (*vide supra*).

Evaluation of these heterocycles for antiproliferative effects and apoptosis induction in human cancer cells resulted in the discovery of uracil-fused pentacycle 8h active in both assays (Figure 2b).¹⁵ The fact that the activity was found in the uracil series was not surprising given that the pyrimidine moiety is capable of both stacking and hydrogen bonding interactions with DNA (an effective demonstration of the somewhat amateurish “like likes like” principle). What was unexpected was that in contrast to most other heterofused library members, this uracil pentacycle was stable toward oxidation under the reaction conditions and was isolated and tested in the dihydropyridine form 8h. Considering the above-discussed requirement for planarity made us question whether 8h worked through topoisomerase and/or DNA targeting. Indeed, it was possible that we serendipitously stumbled upon an unrelated activity residing in this dihydro pentacyclic system. A more plausible explanation was, however, based on the possibility of intracellular oxidation of the dihydropyridine moiety to the planar indenopyridine skeleton 8o, giving rise to the idea that 8h was simply a prodrug. Herein, we report experiments addressed to provide answers to this puzzle. In addition, we describe the construction of a library of uracil-fused pentacycles using compound 8h as a lead and biological evaluation of the library members as potential anticancer agents.

RESULTS AND DISCUSSION

The reaction conditions developed previously for the synthesis of 8h worked well for all aromatic aldehydes tried (Figure 3, Table 1). The requisite aldehydes, indane-1,3-dione, and 6-aminouracil were refluxed in a mixture of acetic acid and ethylene glycol, and the corresponding pentacyclic products precipitated directly from such reaction mixtures. Regardless of whether additional oxygenation was provided by means of an oxygen purge, all products, with the exception of the use of paraformaldehyde leading to unsubstituted planar indenopyridine 25, were in dihydropyridine form (8h–24h). The compounds were analytically pure after a single recrystallization from DMF/H₂O, underscoring the facility of their synthetic

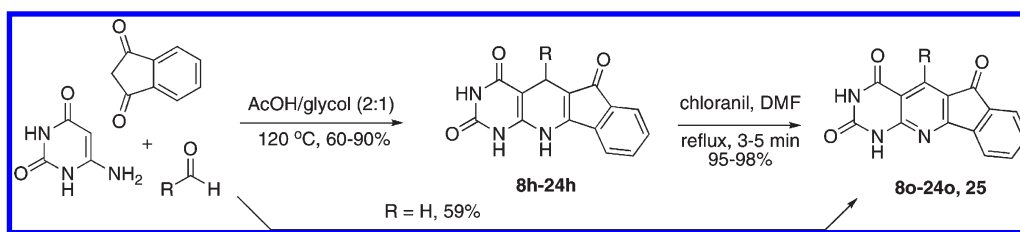


Figure 3. Preparation of the dihydro- and indenopyridine libraries.

preparation. A portion of each of the dihydropyridines was then oxidized to the corresponding indenopyridine **8o–24o**. Chloranil was found to be an excellent oxidizing agent for this purpose, and indenopyridines precipitated from refluxing DMF solutions within a few minutes of the beginning of the reflux in quantitative yields.

The libraries of indenodihydropyridines **8h–24h** and indenopyridines **8o–24o** were then evaluated for their antiproliferative properties¹⁶ in a panel of human cancer cell lines diversely modeling various types of human malignancy: T-cell leukemia, cervical, breast, and lung cancers (Table 1). Additionally, compound pairs that exhibited promising submicromolar potencies were further evaluated in a panel of more challenging cancer models (e.g., apoptosis-resistant): melanoma, glioblastoma, colon, and prostate cancer cell lines (Table 1). In general, the compounds exhibited low micromolar and submicromolar antiproliferative potencies, faring respectably in comparison with the gold standard in this field of research, structurally complex camptothecin (see the average sensitivities toward all cell lines indicated as mean-graph midpoint (MG-MID) values in Table 1). In addition, planar 3,4-dichloro-derivative **15o** and *para*-methylthioether **18o** stand out in displaying two-digit nanomolar potencies toward LoVo colon, U373 glioblastoma, SKMEL-28 melanoma, and Jurkat, U373 glioblastoma cell lines, respectively. Figure 4 provides a visual comparison of antiproliferative potencies between camptothecin and the best analogues from the MCR library.

It is noteworthy that there is a lack of clearly defined SARs in either the dihydro- or pyridine series. Indeed, the variation of antiproliferative activities among the library members encompasses only 2 orders of magnitude and, thus, it appears that modifications of the aldehyde-derived pyridine substituent (R in Figure 3) have no significant impact on activity, while the unsubstituted (R = H in Figure 3) indenopyridine **25** is inactive. While these observations are revealing for further ligand–target structural work, they can be immediately utilized to optimize the druglike properties of library members by incorporating the required pyridine substituents that would enhance drugability while having little effect on activity. This finding also indicated that diversity sites other than the pyridine ring in the molecule should be explored in search of enhanced potencies, such as the indenone subunit. We also attempted to build QSAR models using the semiempirical AM1 method with the entire set of compounds as well as subsets of “h” and “o” only. Unfortunately, no statistically significant correlation with a cross-validation coefficient $Q_2 > 0.4$ was obtained for any QSAR model attempted. It has been reported¹⁷ that DNA/topoisomerase-targeting agents could exhibit useful QSAR correlations using LUMO energy values. Indeed, we found negative LUMO energies for all the compounds in Table 1, indicating that they should be electron acceptors, which could be stabilized by donor DNA base pairs through frontier molecular orbital interactions. However, the preferred geometries (especially for the “o” series) involve the perpendicular orientation of the aldehyde-derived aromatic ring with respect to the tetracyclic framework, and therefore, variations in this substituent have little

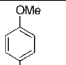
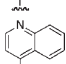
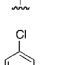
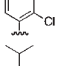
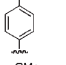
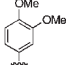
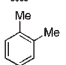
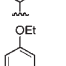
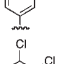
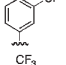
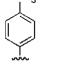
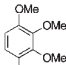
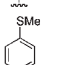
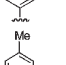
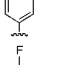
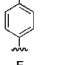
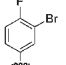
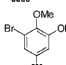
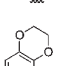
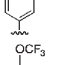
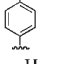
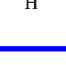

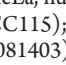

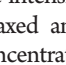
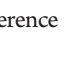


effect on the LUMO energies of these molecules (see the Supporting Information for details).

The biological results in Table 1 also support the hypothesis that dihydropyridines **8h–24h** do not have activity of their own but rather undergo intracellular oxidation to the corresponding planar pyridines **8o–24o**. Indeed, with few exceptions, the antiproliferative potencies within each pair of “h” and “o” analogues are remarkably similar (see, for example, **8h** vs **8o** or **10h** vs **10o**, etc). Exceptions do exist, however. In these cases the oxidized analogues outcompete their dihydro counterpart in each pair by exhibiting higher potencies (see, for example, **11h** vs **11o** or **15h** vs **15o** toward HeLa cells; compare also the MG-MID values for all h/o pairs). It is likely that the intracellular oxidation rates are slow for some dihydropyridines and insufficient amounts of the active “o” counterparts are generated during the course of the assay. Also, utilizing a caspase-3 activation assay performed with Jurkat cells (data not shown), we confirmed that both dihydro and oxidized library members induced cell-killing by triggering apoptosis. Again, the time(s) required for maximum caspase-3 activation and the dose-dependence profiles were similar within “h” and “o” pairs of analogues, indicating that mechanistically the dihydro and oxidized library members were similar.

The investigation of the morphological changes provided further evidence that the effects of both dihydro and oxidized compounds on cultured cells are similar. The U373 cell line was chosen because it displays intrinsic resistance to pro-apoptotic stimuli.¹⁸ We then employed computer-assisted phase-contrast microscopy¹⁹ (quantitative videomicroscopy) to determine whether camptothecin (**1**) and analogue pairs **13h,o** and **18h,o** display cytotoxic or cytostatic effects in this human glioblastoma cell line. Figure 5 shows that camptothecin (**1**) exerts its antiproliferative activity against this *in vitro* cancer primarily through cytostatic effects. While compounds **13h**, **13o**, **18h**, and **18o** also display cytostatic activity, typical features of cytotoxic effects can be observed as well, and they are indicated by the white arrows (Figure 5). Thus, it appears that all four synthetic compounds have a uniform mode of action in this challenging cancer model, which is somewhat different from that of camptothecin.

Because the dihydropyridine library members are stable toward air oxidation and can be stored in DMSO solutions at room temperature without any signs of their conversion to planar indenopyridines, we surmised that cell-free DNA binding and topoisomerase inhibition assays would reveal the mechanistic disparity between the “h” and “o” pentacycles. Fluorescence measurements utilizing major and minor groove binding dyes failed to detect any significant affinity of either “h” or “o” pentacycles toward DNA (data not shown). This was not surprising, as many topoisomerase-targeting agents (e.g., camptothecin) do not have DNA affinity of their own, and thus, we performed DNA relaxation experiments with both topoisomerase I and II. Supercoiled plasmid DNA pGEM1 was incubated with human topoisomerase I and pairs of compounds **18h,o** and **13h,o** at a concentration range of 10–250 μ M (Figure 6).²⁰ Agarose gel electrophoresis monitoring of the plasmid unwinding revealed that

Table 1. In Vitro Antiproliferative GI₅₀ Values

R	#	cell line (in vitro GI ₅₀ antiproliferative values (μM)) ^a								
		HeLa	Jurkat	MCF-7	A-549	LoVo	U373	SKMEL	PC3	MG-MID
	8h	6.9 ± 0.4	0.87 ± 0.04	3.6 ± 0.5	9.2 ± 0.4	2.2 ± 0.3	4.1 ± 0.5	4.8 ± 0.6	3.0 ± 0.5	4.3 ± 0.4
	8o	5.5 ± 0.1	0.96 ± 0.02	2.4 ± 0.5	>10	0.87 ± 0.05	2.4 ± 0.5	4.7 ± 0.3	0.88 ± 0.05	3.5 ± 0.3
	9h	5.6 ± 0.2	8.2 ± 0.4	9.4 ± 0.1	8.6 ± 0.2					8.0 ± 0.2
	9o	7.6 ± 0.1	8.2 ± 0.4	9.5 ± 0.7	>10					8.8 ± 0.4
	10h	0.95 ± 0.07	0.76 ± 0.05	7.0 ± 0.7	7.4 ± 0.5	1.4 ± 0.3	4.2 ± 0.3	3.9 ± 0.5	2.4 ± 0.4	3.5 ± 0.4
	10o	0.89 ± 0.03	0.81 ± 0.03	7.4 ± 0.5	7.8 ± 0.6	2.9 ± 0.2	4.2 ± 0.2	3.5 ± 0.7	2.8 ± 0.3	3.8 ± 0.3
	11h	5.8 ± 0.5	0.96 ± 0.06	9.1 ± 0.1	>10					6.5 ± 0.3
	11o	0.85 ± 0.03	0.49 ± 0.02	6.9 ± 0.1	8.2 ± 0.4					4.1 ± 0.1
	12h	0.60 ± 0.04	0.40 ± 0.01	0.69 ± 0.02	4.8 ± 0.9	0.8 ± 0.3	0.70 ± 0.01	0.86 ± 0.07	>10	2.3 ± 0.3
	12o	0.53 ± 0.04	0.22 ± 0.01	0.75 ± 0.01	0.83 ± 0.06	0.44 ± 0.04	0.6 ± 0.1	0.47 ± 0.02	>10	1.7 ± 0.1
	13h	0.78 ± 0.05	0.19 ± 0.01	0.34 ± 0.03	0.29 ± 0.01	0.49 ± 0.02	0.43 ± 0.03	0.96 ± 0.09	4.2 ± 0.9	0.96 ± 0.08
	13o	0.19 ± 0.01	0.17 ± 0.02	0.19 ± 0.01	0.14 ± 0.01	0.33 ± 0.03	0.50 ± 0.02	0.45 ± 0.07	0.48 ± 0.04	0.31 ± 0.02
	14h	7.4 ± 0.5	0.91 ± 0.05	6.6 ± 0.5	5.8 ± 0.4					5.2 ± 0.3
	14o	5.3 ± 0.1	0.76 ± 0.01	5.6 ± 0.1	6.0 ± 0.7					4.4 ± 0.2
	15h	5.8 ± 0.4	0.35 ± 0.03	0.80 ± 0.01	0.59 ± 0.08	0.46 ± 0.02	0.42 ± 0.03	0.50 ± 0.06	6.2 ± 0.9	1.9 ± 0.9
	15o	0.35 ± 0.04	0.23 ± 0.01	0.74 ± 0.02	0.12 ± 0.01	0.07 ± 0.01	0.08 ± 0.01	0.08 ± 0.01	>10	1.46 ± 0.04
	16h	5.6 ± 0.1	2.2 ± 0.4	1.5 ± 0.7	5.2 ± 0.4					3.6 ± 0.7
	16o	3.8 ± 0.2	0.96 ± 0.02	5.6 ± 0.4	7.8 ± 0.1					4.5 ± 0.2
	17h	0.35 ± 0.01	0.49 ± 0.01	0.48 ± 0.03	0.54 ± 0.02	0.22 ± 0.06	0.26 ± 0.07	0.40 ± 0.03	>10	1.59 ± 0.07
	17o	0.31 ± 0.02	0.47 ± 0.01	0.47 ± 0.01	0.26 ± 0.01	0.35 ± 0.03	0.36 ± 0.02	0.43 ± 0.02	0.9 ± 0.3	0.4 ± 0.3
	18h	0.37 ± 0.01	0.19 ± 0.01	0.36 ± 0.04	0.47 ± 0.01	0.49 ± 0.03	1.1 ± 0.7	1.8 ± 0.9	0.40 ± 0.03	0.6 ± 0.1
	18o	0.17 ± 0.02	0.05 ± 0.01	0.45 ± 0.02	0.61 ± 0.01	0.29 ± 0.04	0.10 ± 0.01	0.23 ± 0.01	0.19 ± 0.03	0.26 ± 0.03
	19h	8.6 ± 0.2	5.6 ± 0.1	7.6 ± 0.2	5.9 ± 0.1					6.9 ± 0.1
	19o	6.4 ± 0.1	1.1 ± 0.1	6.4 ± 0.1	5.8 ± 0.1					4.9 ± 0.2
	20h	>10	>10	>10	>10	4.6 ± 0.2	5.6 ± 0.9	>10	4.0 ± 0.1	8.0 ± 0.5
	20o	>10	7.4 ± 0.6	>10	>10	3.5 ± 0.3	8.7 ± 0.6	>10	9.0 ± 0.8	8.6 ± 0.3
	21h	5.4 ± 0.1	0.99 ± 0.02	5.5 ± 0.7	5.6 ± 0.1					4.4 ± 0.2
	21o	5.6 ± 0.1	0.98 ± 0.01	5.5 ± 0.7	2.8 ± 0.5					3.7 ± 0.3
	22h	3.8 ± 0.1	0.20 ± 0.01	0.78 ± 0.04	0.48 ± 0.02	0.38 ± 0.04	0.37 ± 0.04	0.48 ± 0.06	>10	2.06 ± 0.6
	22o	0.34 ± 0.01	0.17 ± 0.01	0.95 ± 0.07	0.31 ± 0.09	0.35 ± 0.06	0.6 ± 0.1	0.47 ± 0.02	>10	1.6 ± 0.1
	23h	5.4 ± 0.1	6.9 ± 0.1	8.4 ± 0.1	7.8 ± 0.9					7.1 ± 0.3
	23o	8.8 ± 0.4	5.5 ± 0.7	8.5 ± 0.7	7.5 ± 0.4					7.6 ± 0.6
	24h	5.6 ± 0.2	0.96 ± 0.02	5.8 ± 0.4	5.7 ± 0.4					4.5 ± 0.2
	24o	5.8 ± 0.4	0.95 ± 0.04	6.6 ± 0.1	8.0 ± 0.7					5.3 ± 0.2
H	25	>10	>10	>10	>10	9.5 ± 0.9	7.5 ± 0.6	>10	>10	>10
	1	1.3 ± 0.4	0.09 ± 0.01	6.0 ± 0.7	0.20 ± 0.01	0.008 ± 0.002	0.033 ± 0.004	0.047 ± 0.003	0.48 ± 0.02	1.0 ± 0.1

^a HeLa, human cervical cancer (ATCC S3); Jurkat, human T-cell leukemia (TIB-152, E6-1 clone); MCF-7, human mammary carcinoma (DSMZ code ACC115); A-549, human NSCLC (DSMZ code ACC107); Lovo, human colon cancer (DSMZ ACC350); U373, human glioblastoma (ECACC 89081403); SKMEL-28, melanoma (ATCC HTB-72); PC-3, human prostate cancer (DSMZ ACC465).

the intensities of the slower migrating bands (corresponding to the relaxed and possibly nicked DNA) were high across the entire concentration range for the pair **13h** and **13o** (Figure 6). In contrast, reference camptothecin completely inhibited DNA relaxation. The

effects of **18h,o** were similar with the exception of some inhibition at a very high concentration of 250 μM. Because these compounds exhibit antiproliferative properties at submicromolar concentrations, it is unlikely that topoisomerase inhibition at 250 μM has any

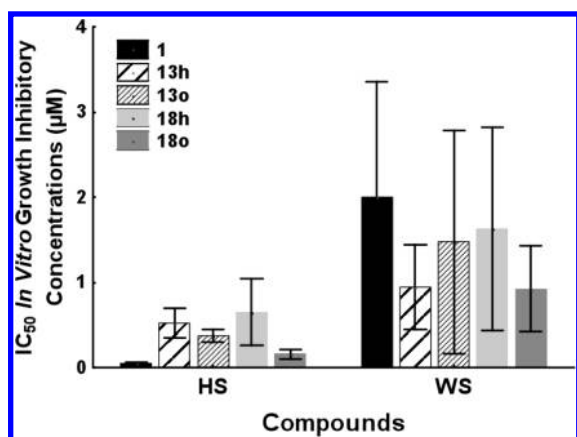


Figure 4. Mean IC_{50} values for camptothecin (**1**) and the best analogues from the MCR library determined on four distinct highly sensitive (HS) versus four distinct weakly sensitive (WS) human cancer cell lines to camptothecin. HS cancer cell lines display mean IC_{50} values for camptothecin $<0.1 \mu\text{M}$ (Jurkat, LoVo, U373, and SKMEL), while WS cancer cell lines display mean IC_{50} values for camptothecin $>0.1 \mu\text{M}$ (HeLa, MCF-7, A-549, and PC-3).

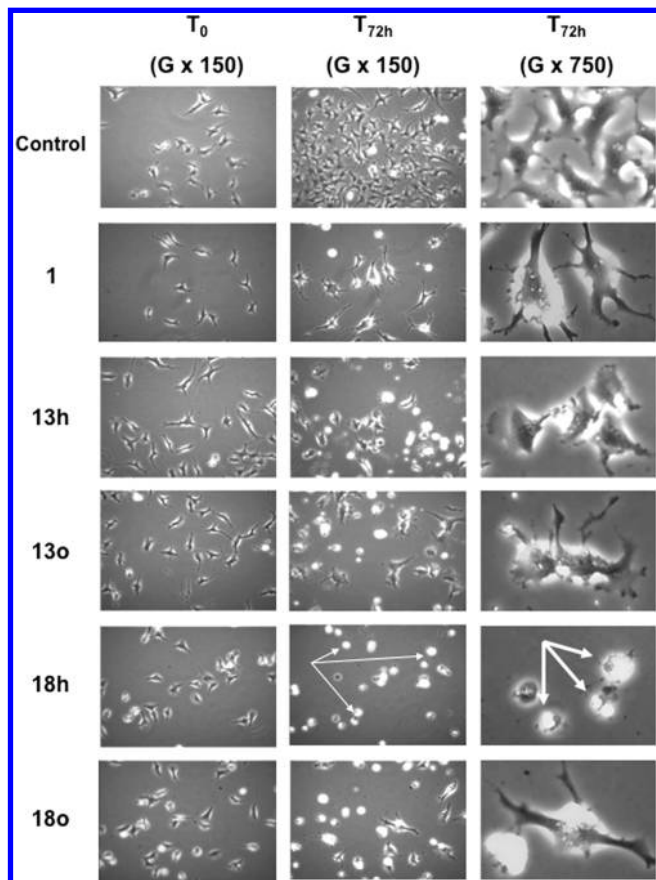


Figure 5. Quantitative videomicroscopy analyses carried out on human U373 glioblastoma cells revealed that camptothecin (**1**) manifests cytostatic features, while compounds **13h**, **13o**, **18h**, and **18o** also display cytotoxic effects in addition to the cytostatic ones. The cytotoxic effects relate to refringent and rounded cells that correspond to dying or dead cells (see the white arrows). Each compound was assayed at its GI_{50} concentration, as revealed by the MTT colorimetric assay on U373 glioblastoma cells (Table 1), i.e. $0.03 \mu\text{M}$ for **1** (camptothecin), $0.4 \mu\text{M}$ for **13h**, $0.5 \mu\text{M}$ for **13o**, $0.1 \mu\text{M}$ for **18h**, and $0.1 \mu\text{M}$ for **18o**.

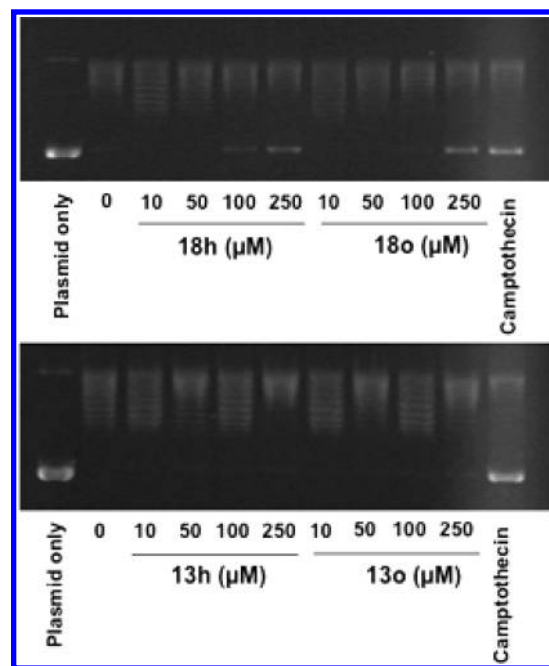


Figure 6. Effects of “h” and “o” pentacycles on relaxation of supercoiled pGEM1 plasmid DNA by topoisomerase I. Camptothecin was used as reference at $100 \mu\text{M}$ concentration. DNA samples were separated by gel electrophoresis.

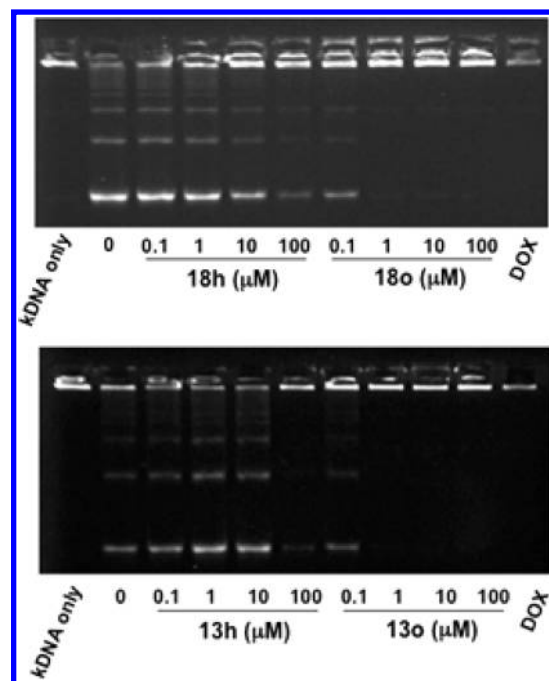


Figure 7. Effects of “h” and “o” pentacycles on decatination of kinetoplast DNA (KDNA) by topoisomerase II. Doxorubicin (DOX) was used as reference at $5 \mu\text{M}$ concentration. DNA samples were separated by gel electrophoresis.

significant contribution to it. In addition, the control experiment showed that none of the compounds had an impact on the plasmid in the absence of Topo I (data not shown). Furthermore, a cleavage complex stabilization assay with compounds **13h,o** and **18h,o** (up to

100 μM) revealed that these compounds do not target topo-I through the cleavage complex stabilization either (data not shown).

Inhibition of topoisomerase II was studied with a decatenation assay (Figure 7). A high level of decatenation was observed with **18h** and **13h** at concentrations of up to at least 10 μM , clearly ruling out the inhibition of topoisomerase II as a possible mechanism accounting for the antiproliferative effect of the dihydropyridine pentacycles. However, complete inhibition of decatenation was induced by 1 μM **18o** and **13o**, and this effect was similar to that for the known topoisomerase II inhibitor doxorubicin used as reference at a concentration of 5 μM . Indeed, inhibition of topoisomerase II by **18o** and **13o** occurs in the concentration range 0.1–1 μM , and this coincides with the antiproliferative GI_{50} values observed by these compounds toward the panel of human cancer cell lines investigated in this work (Table 1). These results provide strong evidence that planar indenopyridines **8o**–**24o** exhibit antiproliferative properties against human cancer cells by inhibiting the activity of topoisomerase II. Altogether, the present study argues that our initially discovered pentacyclic uracil-fused indenodihydropyridine **8h** is a prodrug that undergoes intracellular oxidation to topoisomerase II—targeting planar indenopyridine analogue **8o**.

CONCLUSION

This work represents a successful example of generation of natural-product-mimetic scaffolds through one-step multicomponent synthesis. While analogue preparation by synthetic derivatization of natural products or *de novo* multistep synthetic pathways is an important area of research, the mimetic scaffold approach, practiced in our lab, provides a useful alternative. The camptothecin-inspired 1*H*-indeno[2',1':5,6]pyrido[2,3-*d*]pyrimidine scaffold is accessible by refluxing selected aldehydes, indane-1,3-dione, and 6-aminouracil, all commercially available inexpensive reagents. The products precipitate from the reaction mixtures in dihydropyridine form, and they can be further chemically oxidized or used to treat cancer cells as such. Because of the convenient one-step synthesis, a large number of analogues can be accessed quickly. This could be particularly advantageous in the search for compounds with higher activity or improved druglike properties. In addition to these endeavors, further work in this area will also include efforts aimed at better mechanistic understanding of topoisomerase II targeting by indenopyridines, i.e. whether it is classical catalytic inhibition of the enzyme or stabilization of covalent DNA-topoisomerase II cleavage complexes. Insights gleaned in these investigations will lead to designed analogues, which should be accessible again through a one-step synthesis.

EXPERIMENTAL SECTION

All aldehydes, indane-1,3-dione, 6-aminouracil, chloranil (TCQ), acetic acid, and ethylene glycol were purchased from commercial sources and used without purification. The reactions were carried out in open to the atmosphere vessels. ^1H and ^{13}C NMR spectra were recorded on a JEOL 300 MHz spectrometer. MS analyses were performed at the Mass Spectrometry Facility, University of New Mexico. The synthesized compounds are at least 95% pure according to HPLC and elemental analysis.

General Procedure for the Synthesis of Compounds 8h–24h and 25. The mixture of a selected aldehyde (0.8 mmol), 6-aminouracil (0.76 mmol), and indane-1,3-dione (0.8 mmol) was suspended in 6 mL of solvent (2:1 mixture of acetic acid and ethylene glycol). The reaction suspension slowly converts into a yellow solution upon heating at 120 $^\circ\text{C}$, and usually after 2 h a bright orange precipitate starts to form. After 4 h of heating the reaction mixture is cooled to room temperature and the orange

precipitate is filtered off. It is then washed with 15 mL of ethanol followed by 3 mL of diethyl ether. Yields are usually in the 60–90% range. After recrystallization from DMF/ H_2O the products are 95% pure according to HPLC and elemental analysis.

5-(4-Methoxyphenyl)-5,11-dihydro-1*H*-indeno[2',1':5,6]pyrido[2,3-*d*]pyrimidine-2,4,6(3*H*)-trione (8h). 72%; ^1H NMR (DMSO- d_6) δ : 3.67 (s, 3H), 4.61 (s, 1H), 6.76 (d, J = 9.5, 2H), 7.13 (d, J = 9.8 Hz, 2H), 7.25 (d, J = 7.9 Hz, 1H), 7.32 (d, J = 8.6 Hz, 1H), 7.40 (m, 2H), 10.11 (bs, 1H), 10.29 (bs, 1H), 10.89 (bs, 1H); ^{13}C NMR (DMSO- d_6) δ : 191.5, 163.4, 158.3, 153.9, 150.4, 145.0, 138.1, 136.5, 133.2, 132.7, 130.9, 129.4, 129.2, 123.4, 121.4, 119.5, 114.0, 110.5, 91.8, 55.5; HRMS m/z (ESI) calcd for $\text{C}_{21}\text{H}_{15}\text{N}_3\text{O}_4 + \text{Na}^+$ 396.0960, found 396.0978.

5-(4-Quinolonyl)-5,11-dihydro-1*H*-indeno[2',1':5,6]pyrido[2,3-*d*]pyrimidine-2,4,6(3*H*)-trione (9h). 90%; ^1H NMR (DMSO- d_6) δ : 5.6 (s, 1H), 7.17 (d, J = 7.7 Hz, 1H), 7.33 (d, J = 5.8 Hz, 1H), 7.40 (d, J = 6.3 Hz, 4H), 7.67 (d, J = 6.3 Hz, 1H), 7.74 (d, J = 8.3 Hz, 1H), 7.99 (d, J = 8.5 Hz, 1H), 8.66 (d, J = 9.0 Hz, 1H), 8.77 (d, J = 5.2 Hz, 1H); ^{13}C NMR (DMSO- d_6) δ : 191.1, 172.7, 163.6, 153.7, 151.2, 150.5, 150.2, 147.5, 146.4, 133.1, 132.7, 131.1, 126.6, 125.5, 121.7, 121.5, 121.3, 119.8, 109.8, 91.8, 63.5, 21.6, 21.4; HRMS m/z (ESI) calcd for $\text{C}_{23}\text{H}_{14}\text{N}_4\text{O}_3 + \text{H}^+$ 395.1154, found 395.1158.

5-(2,4-Dichlorophenyl)-5,11-dihydro-1*H*-indeno[2',1':5,6]pyrido[2,3-*d*]pyrimidine-2,4,6(3*H*)-trione (10h). 70%; ^1H NMR (DMSO- d_6) δ : 5.07 (s, 1H), 7.24–7.45 (m, 10H), 10.18 (bs, 1H), 10.81 (bs, 1H). ^{13}C NMR (DMSO- d_6) δ : 191.1, 154.3, 150.6, 145.7, 142.0, 136.3, 134.5, 133.2, 131.8, 131.2, 128.9, 127.7, 126.1, 122.6, 121.4, 119.7, 111.9, 108.7, 90.9, 32.4; HRMS m/z (ESI) calcd for $\text{C}_{20}\text{H}_{11}\text{Cl}_2\text{N}_3\text{O}_3 + \text{Na}^+$ 434.0075, found 434.0086.

5-(4-Isopropylphenyl)-5,11-dihydro-1*H*-indeno[2',1':5,6]pyrido[2,3-*d*]pyrimidine-2,4,6(3*H*)-trione (11h). 77%; ^1H NMR (DMSO- d_6) δ : 1.16 (d, J = 6.0 Hz, 6H), 2.80 (hp, J = 7.4 Hz, 1H), 4.68 (s, 1H), 7.10 (d, J = 8.2 Hz, 2H), 7.15 (d, J = 9 Hz, 2H), 7.28–7.45 (m, 4H), 10.78 (bs, 1H); ^{13}C NMR (DMSO- d_6) δ : 191.5, 163.6, 153.9, 150.3, 146.9, 145.1, 143.5, 136.7, 133.3, 132.7, 130.9, 128.1, 126.5, 121.4, 119.4, 110.5, 91.7, 72.3, 33.8, 33.6, 33.5, 24.5, 24.3; HRMS m/z (ESI) calcd for $\text{C}_{23}\text{H}_{19}\text{N}_3\text{O}_3 + \text{H}^+$ 386.1505, found 386.1517.

5-(3,4-Dimethoxyphenyl)-5,11-dihydro-1*H*-indeno[2',1':5,6]pyrido[2,3-*d*]pyrimidine-2,4,6(3*H*)-trione (12h). 55%; ^1H NMR (DMSO- d_6) δ : 3.70 (s, 3H), 3.83 (s, 3H), 6.83 (d, J = 2.2 Hz, 1H), 6.92 (d, J = 2.1 Hz, 2H), 7.61 (d, J = 2.5 Hz, 2H), 7.75 (m, 1H), 7.82 (d, J = 7.3 Hz, 1H), 11.28 (bs, 1H), 12.17 (bs, 1H); ^{13}C NMR (DMSO- d_6) δ : 191.4, 163.5, 153.6, 150.5, 149.1, 148.3, 145.1, 138.6, 136.7, 133.3, 132.7, 130.9, 121.6, 120.2, 119.4, 113.2, 112.2, 110.5, 91.8, 56.2, 33.7, 33.5; HRMS m/z (ESI) calcd for $\text{C}_{22}\text{H}_{17}\text{N}_3\text{O}_5 + \text{Na}^+$ 426.1066, found 426.1059.

5-(3,4-Dimethylphenyl)-5,11-dihydro-1*H*-indeno[2',1':5,6]pyrido[2,3-*d*]pyrimidine-2,4,6(3*H*)-trione (13h). 90%; ^1H NMR (DMSO- d_6) δ : 2.12 (s, 3H), 2.14 (s, 3H), 4.63 (s, 1H), 6.96 (s, 2H), 7.02 (s, 1H), 7.25–7.43 (m, 4H), 10.01 (bs, 1H), 10.77 (bs, 1H); ^{13}C NMR (DMSO- d_6) δ : 191.4, 163.3, 153.7, 150.3, 145.0, 143.3, 136.5, 135.9, 134.4, 133.2, 132.7, 129.8, 129.3, 125.6, 121.3, 119.3, 119.6, 33.8, 33.6, 19.9, 19.3; HRMS m/z (ESI) calcd for $\text{C}_{22}\text{H}_{17}\text{N}_3\text{O}_3 + \text{Na}^+$ 394.1168, found 394.1162.

5-(4-Ethoxyphenyl)-5,11-dihydro-1*H*-indeno[2',1':5,6]pyrido[2,3-*d*]pyrimidine-2,4,6(3*H*)-trione (14h). 62%; ^1H NMR (DMSO- d_6) δ : 1.26 (t, J = 7.3 Hz, 3H), 3.96 (d, J = 6.1 Hz, 2H), 4.60 (s, 1H), 6.76 (d, J = 8.5 Hz, 2H), 7.14 (d, J = 8.6 Hz, 2H), 7.15–7.43 (m, 4H), 10.09 (bs, 1H), 10.89 (bs, 1H); ^{13}C NMR (DMSO- d_6) δ : 191.5, 163.4, 157.6, 153.8, 150.4, 144.9, 137.9, 136.5, 133.2, 132.7, 131.9, 129.2, 121.4, 119.5, 114.4, 110.5, 91.9, 63.4, 33.2, 15.3; HRMS m/z (ESI) calcd for $\text{C}_{22}\text{H}_{17}\text{N}_3\text{O}_4 + \text{Na}^+$ 410.1117, found 410.1135.

5-(3,4-Dichlorophenyl)-5,11-dihydro-1*H*-indeno[2',1':5,6]pyrido[2,3-*d*]pyrimidine-2,4,6(3*H*)-trione (15h). 68%; ^1H NMR (DMSO- d_6) δ : 4.77 (s, 1H), 7.27–7.47 (m, 7H), 10.42 (bs, 1H), 10.98 (bs, 1H); ^{13}C NMR (DMSO- d_6) δ : 191.2, 163.2, 154.2, 150.1, 146.8, 145.6,

133.3, 132.6, 131.2, 130.6, 130.2, 129.5, 128.6, 121.4, 109.1, 90.9; HRMS m/z (ESI) calcd for $C_{20}H_{11}C_{12}N_3O_3 + Na^+$ 434.0075, found 434.0063.

5-[4-(Trifluoromethyl)phenyl]-5,11-dihydro-1H-indeno[2',1':5,6]pyrido[2,3-d]pyrimidine-2,4,6(3H)-trione (**16h**). 64%; 1H NMR (DMSO- d_6) δ : 4.83 (s, 1H), 7.40–7.47 (m, 4H), 7.53 (d, $J = 8.5$ Hz, 2H), 7.56 (d, $J = 8.2$ Hz, 2H), 10.69 (bs, 1H); ^{13}C NMR (DMSO- d_6) δ : 191.3, 163.4, 154.4, 150.6, 145.7, 136.5, 133.1, 132.7, 131.1, 129.2, 125.5, 121.5, 119.6, 109.4, 90.8; HRMS m/z (ESI) calcd for $C_{21}H_{10}F_3N_3O_3 + Na^+$ 434.0728, found 434.0744.

5-(2,3,4-Trimethoxyphenyl)-5,11-dihydro-1H-indeno[2',1':5,6]pyrido[2,3-d]pyrimidine-2,4,6(3H)-trione (**17h**). 68%; 1H NMR (DMSO- d_6) δ : 3.67 (s, 3H), 3.71 (s, 3H), 3.83 (s, 3H), 4.78 (s, 1H), 6.63 (d, $J = 9.8$ Hz, 1H), 6.79 (d, $J = 9.9$ Hz, 1H), 7.22 (d, $J = 7.3$ Hz, 2H), 7.31–7.42 (m, 4H), 10.79 (bs, 1H); ^{13}C NMR (DMSO- d_6) δ : 191.2, 163.2, 153.9, 152.7, 152.1, 150.5, 145.2, 142.2, 136.7, 133.4, 132.5, 131.7, 130.8, 124.6, 121.2, 119.1, 119.0, 110.4, 108.2, 92.1, 60.8, 56.4; HRMS m/z (ESI) calcd for $C_{23}H_{19}N_3O_6 + Na^+$ 456.1172, found 456.1191.

5-[4-(Methylsulfanyl)phenyl]-5,11-dihydro-1H-indeno[2',1':5,6]pyrido[2,3-d]pyrimidine-2,4,6(3H)-trione (**18h**). 61%; 1H NMR (DMSO- d_6) δ : 2.39 (s, 3H), 4.66 (s, 1H), 7.14–7.39 (m, 8H), 10.08 (bs, 1H), 10.79 (bs, 1H); ^{13}C NMR (DMSO- d_6) δ : 191.6, 163.6, 154.0, 150.5, 145.4, 142.9, 136.4, 136.1, 133.2, 132.7, 131.0, 129.0, 126.8, 121.4, 119.4, 110.0, 91.7, 33.6; HRMS m/z (ESI) calcd for $C_{21}H_{15}N_3O_3S + Na^+$ 412.0732, found 412.0730.

5-(4-Methylphenyl)-5,11-dihydro-1H-indeno[2',1':5,6]pyrido[2,3-d]pyrimidine-2,4,6(3H)-trione (**19h**). 76%; 1H NMR (DMSO- d_6) δ : 2.21 (s, 3H), 4.66 (s, 1H), 7.01 (d, $J = 9.2$ Hz, 2H), 7.14 (d, $J = 9.5$ Hz, 2H), 7.25–7.47 (m, 4H), 10.02 (bs, 1H), 10.78 (bs, 1H); ^{13}C NMR (DMSO- d_6) δ : 191.4, 163.6, 153.9, 150.6, 145.2, 142.9, 136.5, 135.7, 133.3, 132.7, 130.9, 129.1, 128.1, 121.4, 119.3, 110.5, 91.9, 21.0; HRMS m/z (ESI) calcd for $C_{21}H_{15}N_3O_3 + Na^+$ 380.1011, found 380.1022.

5-(4-Fluorophenyl)-5,11-dihydro-1H-indeno[2',1':5,6]pyrido[2,3-d]pyrimidine-2,4,6(3H)-trione (**20h**). 67%; 1H NMR (DMSO- d_6) δ : 4.69 (s, 1H), 7.02 (t, $J = 9.2$ Hz, 2H), 7.28–7.44 (m, 6H), 10.13 (bs, 1H), 10.85 (bs, 1H); ^{13}C NMR (DMSO- d_6) δ : 191.4, 163.4, 154.0, 150.4, 145.2, 141.9, 136.3, 133.1, 132.7, 131.0, 130.0, 121.4, 119.5, 119.4, 115.3, 110.0, 91.5; HRMS m/z (ESI) calcd for $C_{20}H_{12}FN_3O_3 + Na^+$ 382.0604, found 384.0746.

5-(3-Bromo-4-fluorophenyl)-5,11-dihydro-1H-indeno[2',1':5,6]pyrido[2,3-d]pyrimidine-2,4,6(3H)-trione (**21h**). 68%; 1H NMR (DMSO- d_6) δ : 4.70 (s, 1H), 7.20–7.52 (m, 7H), 10.84 (bs, 1H); ^{13}C NMR (DMSO- d_6) δ : 191.2, 175.8, 163.6, 154.4, 150.3, 145.6, 143.8, 133.1, 131.1, 121.6, 119.6, 116.8, 109.2, 108.2, 91.0; HRMS m/z (ESI) calcd for $C_{21}H_{11}BrFN_3O_3 + Na^+$ 461.9866, found 461.9845.

5-(3-Bromo-4,5-dimethoxyphenyl)-5,11-dihydro-1H-indeno[2',1':5,6]pyrido[2,3-d]pyrimidine-2,4,6(3H)-trione (**22h**). 61%; 1H NMR (DMSO- d_6) δ : 3.65 (s, 3H), 3.77 (s, 3H), 4.66 (s, 1H), 6.89 (s, 1H), 6.99 (s, 1H), 7.29–7.47 (m, 4H), 10.21 (bs, 1H), 10.96 (bs, 1H); ^{13}C NMR (DMSO- d_6) δ : 191.4, 163.5, 154.2, 153.4, 150.4, 145.5, 144.6, 143.1, 136.2, 133.1, 132.8, 131.1, 123.2, 121.5, 119.8, 116.8, 112.9, 109.3, 90.8, 60.5, 56.5; HRMS m/z (ESI) calcd for $C_{22}H_{16}BrN_3O_5 + Na^+$ 504.0171, found 504.0180.

5-(2,3-Dihydro-1,4-benzodioxin-6-yl)-5,11-dihydro-1H-indeno[2',1':5,6]pyrido[2,3-d]pyrimidine-2,4,6(3H)-trione (**23h**). 73%; 1H NMR (DMSO- d_6) δ : 4.14 (m, 4H), 4.53 (s, 1H), 6.67 (s, 3H), 7.25–7.47 (m, 4H), 10.15 (bs, 1H), 10.91 (bs, 1H); ^{13}C NMR (DMSO- d_6) δ : 191.5, 163.4, 153.8, 150.4, 145.0, 143.3, 142.4, 139.0, 136.4, 133.1, 132.7, 130.9, 121.4, 120.8, 119.6, 117.1, 110.3, 91.7, 64.6; HRMS m/z (ESI) calcd for $C_{22}H_{15}N_3O_5$ 424.0909, found 424.0935.

5-[4-(Trifluoromethoxy)phenyl]-5,11-dihydro-1H-indeno[2',1':5,6]pyrido[2,3-d]pyrimidine-2,4,6(3H)-trione (**24h**). 56%; 1H NMR (DMSO- d_6) δ : 4.75 (s, 1H), 7.18 (d, $J = 7.7$ Hz, 2H), 7.33 (d, $J = 7.4$ Hz, 2H), 7.38 (d, $J = 7.2$ Hz, 4H), 10.8 (s, 1H). ^{13}C NMR (DMSO- d_6) δ : 191.3, 163.4,

154.2, 154.2, 150.3, 147.3, 145.3, 144.9, 136.3, 133.1, 132.7, 131.0, 129.9, 121.4, 120.9, 119.6, 119.4, 109.7, 91.2, 33.9, 33.7; HRMS m/z (ESI) calcd for $C_{21}H_{12}F_3N_3O_4 + Na^+$ 450.0678, found 450.0682.

1H-Indeno[2',1':5,6]pyrido[2,3-d]pyrimidine-2,4,6(3H)-trione (**25**). 59%; 1H NMR (DMSO- d_6) δ : 7.59 (dd, $J = 6.7$ Hz, 1H), 7.67–7.75 (m, 3H), 8.16 (s, 1H). ^{13}C NMR (DMSO- d_6) δ : 189.3, 169.8, 162.3, 157.5, 150.7, 141.6, 136.5, 136.0, 133.3, 131.9, 124.2, 123.5, 122.2, 109.6; HRMS m/z (ESI) calcd for $C_{14}H_7N_3O_3 + H^+$ 266.0566, found 266.0550.

General Procedure for the Synthesis of Oxidized Compounds 80–240. To a selected dihydro compound (0.082 mmol) in hot DMF (1 mL) was added chloranil (0.085 mmol) in one portion. The reaction mixture then was heated at reflux for 4 min, and 0.1 mL of water was added. The mixture was reheated again and then cooled to room temperature. The yellow precipitate was formed upon standing for 10 min at room temperature. The precipitate was filtered on a glass filter and rinsed with 3 mL of ethanol followed by 1 mL of diethyl ether. Yellow precipitates were obtained in quantitative yields and displayed purity higher than 95% by HPLC and elemental analysis.

5-(4-Methoxyphenyl)-1H-indeno[2',1':5,6]pyrido[2,3-d]pyrimidine-2,4,6(3H)-trione (**80**). 97%; 1H NMR (DMSO- d_6) δ : 3.83 (s, 3H), 6.92 (dd, $J = 7.4$ Hz, 2H), 7.23 (dd, $J = 7.6$ Hz, 2H), 7.61 (m, 2H), 7.76 (d, $J = 4.3$ Hz, 1H), 7.82 (t, $J = 5.9$ Hz, 1H), 11.28 (bs, 1H), 12.18 (bs, 1H); ^{13}C NMR (DMSO- d_6) δ : 189.5, 168.9, 161.8, 159.8, 158.1, 152.5, 150.5, 140.7, 136.6, 135.9, 133.4, 130.3, 126.4, 123.9, 122.0, 113.0, 112.8, 107.4, 55.6; HRMS m/z (ESI) calcd for $C_{21}H_{13}N_3O_4 + Na^+$ 394.0804, found 394.0812.

5-(4-Quinolinyloxy)-1H-indeno[2',1':5,6]pyrido[2,3-d]pyrimidine-2,4,6(3H)-trione (**90**). 95%; 1H NMR (DMSO- d_6) δ : 7.53–7.90 (m, 10H), 8.21 (d, $J = 8.3$ Hz, 1H), 9.08 (d, $J = 4.7$ Hz, 1H), 11.4 (bs, 1H), 12.5 (bs, 1H). ^{13}C NMR (DMSO- d_6) δ : 188.5, 169.2, 161.5, 158.3, 150.4, 148.6, 148.5, 144.6, 141.0, 136.5, 136.3, 133.7, 131.3, 128.1, 127.3, 126.8, 126.4, 124.2, 122.4, 121.5, 121.3, 120.3, 108.0; HRMS m/z (ESI) calcd for $C_{23}H_{24}N_4O_3 + H^+$ 393.0988, found 393.1001.

5-(2,4-Dichlorophenyl)-1H-indeno[2',1':5,6]pyrido[2,3-d]pyrimidine-2,4,6(3H)-trione (**100**). 95%; 1H NMR (DMSO- d_6) δ : 7.32 (s, 1H), 7.47 (s, 1H), 7.65 (s, 4H), 7.88 (s, 1H), 11.5 (bs, 1H), 12.4 (bs, 1H); ^{13}C NMR (DMSO- d_6) δ : 188.6, 169.1, 161.5, 158.1, 150.3, 147.0, 140.9, 140.1, 136.4, 136.3, 133.7, 132.3, 130.9, 128.5, 127.3, 124.3, 122.4, 121.0, 107.4; HRMS m/z (ESI) calcd for $C_{20}H_9Cl_2N_3O_3 + H^+$ 410.0099, found 410.0113.

5-(4-Isopropylphenyl)-1H-indeno[2',1':5,6]pyrido[2,3-d]pyrimidine-2,4,6(3H)-trione (**110**). 96%; 1H NMR (DMSO- d_6) δ : 1.28 (d, $J = 7.3$ Hz, 6H), 2.90 (m, 1H), 7.19 (d, $J = 9.2$ Hz, 2H), 7.23 (d, $J = 8.9$ Hz, 2H), 7.61 (d, $J = 8.9$ Hz, 2H), 7.77 (d, $J = 8.2$ Hz, 2H), 7.95 (s, 1H), 10.24 (bs, 1H), 11.28 (bs, 1H), 12.21 (bs, 1H); ^{13}C NMR (DMSO- d_6) δ : 188.7, 168.9, 161.5, 158.0, 152.6, 150.4, 148.3, 144.6, 140.7, 136.6, 135.9, 133.5, 131.9, 128.5, 125.4, 123.9, 122.1, 121.3, 107.4, 33.8, 24.5; HRMS m/z (ESI) calcd for $C_{23}H_{17}N_3O_3 + Na^+$ 406.1168, found 406.1184.

5-(3,4-Dimethoxyphenyl)-1H-indeno[2',1':5,6]pyrido[2,3-d]pyrimidine-2,4,6(3H)-trione (**120**). 97%; 1H NMR (DMSO- d_6) δ : 3.70 (s, 3H), 3.83 (s, 3H), 6.80 (dd, $J = 9.1$ Hz, 3H), 7.61 (d, $J = 47.9$ Hz, 2H), 7.82 (d, $J = 7.9$ Hz), 11.29 (s, 1H), 12.18 (s, 1H); ^{13}C NMR (DMSO- d_6) δ : 188.7, 168.8, 161.6, 158.0, 152.4, 150.4, 149.3, 148.0, 140.6, 136.6, 135.9, 133.4, 126.7, 123.9, 122.0, 121.5, 121.2, 112.2, 111.0, 107.4, 56.1, 56.0; HRMS m/z (ESI) calcd for $C_{22}H_{15}N_3O_5 + Na^+$ 424.0909, found 424.0899.

5-(3,4-Dimethylphenyl)-1H-indeno[2',1':5,6]pyrido[2,3-d]pyrimidine-2,4,6(3H)-trione (**130**). 95%; 1H NMR (DMSO- d_6) δ : 2.23 (s, 3H), 2.31 (s, 3H), 6.98 (d, $J = 8.3$ Hz, 1H), 7.02 (s, 1H), 7.12 (d, $J = 7.9$ Hz, 1H), 7.60 (d, $J = 7.6$ Hz, 1H), 7.64 (t, $J = 8.3$ Hz, 1H), 7.76 (d, $J = 7.3$ Hz, 2H), 11.27 (bs, 1H), 12.20 (bs, 1H); ^{13}C NMR (DMSO- d_6) δ : 188.7, 168.9, 161.5, 158.1, 152.7, 150.4, 140.7, 136.6, 136.2, 135.9, 135.0, 133.1, 129.3, 128.8, 125.9, 123.9, 122.0, 121.1, 107.4, 20.0; HRMS m/z (ESI) calcd for $C_{22}H_{15}N_3O_3 + Na^+$ 392.1011, found 392.1023.

5-(4-Ethoxyphenyl)-1H-indeno[2',1':5,6]pyrido[2,3-d]pyrimidine-2,4,6(3H)-trione (**140**). 96%; 1H NMR (DMSO- d_6) δ : 1.39 (t, $J = 7.3$ Hz, 3H), 4.07 (q, $J = 6.8$ Hz, 2H), 6.89 (d, $J = 8.8$ Hz, 2H), 7.19 (d, $J = 9.3$ Hz,

2H), 7.61 (s, 1H), 7.76 (t, $J = 4.8$ Hz, 1H), 7.83 (d, $J = 7.6$ Hz, 2H), 11.27 (bs, 1H), 12.18 (bs, 1H); ^{13}C NMR (DMSO- d_6) δ : 188.8, 168.9, 161.7, 159.1, 158.1, 152.6, 150.4, 140.7, 136.6, 135.9, 135.8, 133.4, 130.3, 126.2, 123.9, 122.0, 121.1, 113.4, 113.2, 107.4, 63.5; HRMS m/z (ESI) calcd for $\text{C}_{22}\text{H}_{15}\text{N}_3\text{O}_4 + \text{Na}^+$ 408.0960, found 408.0945.

5-(3,4-Dichlorophenyl)-1H-indeno[2',1':5,6]pyrido[2,3-d]pyrimidine-2,4,6(3H)-trione (**15o**). 98%; ^1H NMR (DMSO- d_6) δ : 7.27 (d, $J = 7.0$ Hz, 2H), 7.63 (d, $J = 1.5$ Hz, 3H), 7.77 (d, $J = 19.5$ Hz, 2H), 11.42 (bs, 1H), 12.31 (bs, 1H); ^{13}C NMR (DMSO- d_6) δ : 188.7, 168.8, 161.8, 158.0, 150.3, 148.8, 140.7, 136.6, 136.1, 135.7, 133.6, 131.0, 130.4, 130.3, 130.0, 129.0, 124.1, 122.2, 121.1, 109.2; HRMS m/z (ESI) calcd for $\text{C}_{20}\text{H}_9\text{Cl}_2\text{N}_3\text{O}_3 + \text{Na}^+$ 431.9919, found 431.9914.

5-[4-(Trifluoromethyl)phenyl]-1H-indeno[2',1':5,6]pyrido[2,3-d]pyrimidine-2,4,6(3H)-trione (**16o**). 95%; ^1H NMR (DMSO- d_6) δ : 7.41 (s, 2H), 7.51 (s, 2H), 7.84 (s, 4H), 11.40 (bs, 1H), 12.32 (bs, 1H). ^{13}C NMR (DMSO- d_6) δ : 188.7, 168.9, 161.7, 158.0, 150.4, 150.2, 140.7, 140.1, 139.6, 136.5, 136.1, 133.6, 129.3, 129.1, 128.4, 124.6, 124.1, 122.2, 121.0, 107.2; HRMS m/z (ESI) calcd for $\text{C}_{21}\text{H}_{10}\text{F}_3\text{N}_3\text{O}_3 + \text{Na}^+$ 432.0572, found 432.0565.

5-(2,3,4-Trimethoxyphenyl)-1H-indeno[2',1':5,6]pyrido[2,3-d]pyrimidine-2,4,6(3H)-trione (**17o**). 99%; ^1H NMR (DMSO- d_6) δ : 3.35 (s, 3H), 3.74 (s, 3H), 3.86 (s, 3H), 6.79 (s, 3H), 7.63 (s, 1H), 7.73 (d, $J = 8.7$ Hz, 1H), 7.84 (d, $J = 8.8$ Hz, 1H), 11.32 (bs, 1H), 12.22 (bs, 1H); ^{13}C NMR (DMSO- d_6) δ : 188.8, 178.1, 161.6, 157.9, 154.1, 150.7, 148.9, 141.0, 136.6, 123.5, 122.2, 121.7, 107.5, 61.0, 56.4; HRMS m/z (ESI) calcd for $\text{C}_{23}\text{H}_{17}\text{N}_3\text{O}_6 + \text{Na}^+$ 454.1015, found 454.1003.

5-[4-(Methylsulfanyl)phenyl]-1H-indeno[2',1':5,6]pyrido[2,3-d]pyrimidine-2,4,6(3H)-trione (**18o**). 97%; ^1H NMR (DMSO- d_6) δ : 2.51 (s, 3H), 7.23 (s, 4H), 7.61 (d, $J = 7.0$ Hz, 2H), 7.76 (t, $J = 7.0$ Hz, 1H), 7.83 (d, $J = 7.9$ Hz, 1H), 11.32 (bs, 1H), 12.22 (bs, 1H); ^{13}C NMR (DMSO- d_6) δ : 188.6, 168.9, 161.7, 158.1, 151.9, 150.4, 140.7, 138.5, 136.6, 136.0, 133.7, 131.0, 129.6, 124.7, 124.0, 122.1, 121.1, 107.2, 21.3; HRMS m/z (ESI) calcd for $\text{C}_{21}\text{H}_{13}\text{N}_3\text{O}_3\text{S} + \text{Na}^+$ 410.0575, found 410.0580.

5-(4-Methylphenyl)-1H-indeno[2',1':5,6]pyrido[2,3-d]pyrimidine-2,4,6(3H)-trione (**19o**). 96%; ^1H NMR (DMSO- d_6) δ : 2.40 (s, 3H), 7.17 (s, 4H), 7.60–7.83 (m, 4H), 10.21 (bs, 1H), 11.28 (bs, 1H), 12.20 (bs, 1H); ^{13}C NMR (DMSO- d_6) δ : 188.7, 168.9, 161.6, 158.0, 152.6, 144.6, 140.7, 136.6, 133.4, 131.7, 128.4, 123.9, 122.1, 121.3, 107.4, 21.6; HRMS m/z (ESI) calcd for $\text{C}_{21}\text{H}_{13}\text{N}_3\text{O}_3 + \text{Na}^+$ 378.0855, found 378.0867.

5-(4-Fluorophenyl)-1H-indeno[2',1':5,6]pyrido[2,3-d]pyrimidine-2,4,6(3H)-trione (**20o**). 95%; ^1H NMR (DMSO- d_6) δ : 7.20 (dd, $J = 9.8$ Hz, 2 Hz), 7.31 (dd, $J = 6.1$ Hz, 2 Hz), 7.61 (t, $J = 6.4$ Hz, 2H), 7.76 (dt, $J = 7.9$ Hz, 1H), 7.83 (d, $J = 8.5$ Hz, 1H), 11.34 (bs, 1H), 12.25 (bs, 1H); ^{13}C NMR (DMSO- d_6) δ : 188.8, 168.8, 161.7, 158.0, 151.2, 150.4, 140.7, 136.0, 133.0, 130.7, 124.0, 122.1, 121.2, 114.7, 107.4; HRMS m/z (ESI) calcd for $\text{C}_{20}\text{H}_{10}\text{FN}_3\text{O}_3 + \text{Na}^+$ 382.0604, found 382.0617.

5-(3-Bromo-4-fluorophenyl)-1H-indeno[2',1':5,6]pyrido[2,3-d]pyrimidine-2,4,6(3H)-trione (**21o**). 96%; ^1H NMR (DMSO- d_6) δ : 7.38 (m, 1H), 7.65–7.95 (m, 6H), 11.40 (bs, 1H), 12.30 (bs, 1H); ^{13}C NMR (DMSO- d_6) δ : 192.3, 188.8, 170.8, 168.8, 161.8, 158.0, 150.3, 140.7, 140.1, 133.6, 132.8, 130.2, 124.2, 122.2, 121.2, 116.2, 107.4; HRMS m/z (ESI) calcd for $\text{C}_{20}\text{H}_9\text{BrFN}_3\text{O}_3 + \text{H}^+$ 437.9890, found 437.1978.

5-(3-Bromo-4,5-dimethoxyphenyl)-1H-indeno[2',1':5,6]pyrido[2,3-d]pyrimidine-2,4,6(3H)-trione (**22o**). 99%; ^1H NMR (DMSO- d_6) δ : 3.77 (s, 3H), 3.83 (s, 3H), 7.04 (s, 1H), 7.08 (s, 1H), 7.63 (d, $J = 4.0$ Hz, 2H), 7.77 (m, 1H), 7.84 (d, $J = 7.9$ Hz, 1H), 11.36 (bs, 1H), 12.26 (bs, 1H); ^{13}C NMR (DMSO- d_6) δ : 188.7, 168.8, 161.6, 157.9, 152.9, 150.4, 145.7, 140.7, 136.6, 133.6, 132.1, 124.1, 122.1, 121.2, 115.9, 113.4, 107.4, 60.7, 56.6; HRMS m/z (ESI) calcd for $\text{C}_{22}\text{H}_{14}\text{BrN}_3\text{O}_5 + \text{H}^+$ 502.0015, found 504.0020.

5-(2,3-Dihydro-1,4-benzodioxin-6-yl)-1H-indeno[2',1':5,6]pyrido[2,3-d]pyrimidine-2,4,6(3H)-trione (**23o**). 95%; ^1H NMR (DMSO- d_6) δ : 4.30 (m, 4H), 6.77 (m, 3H), 7.61 (d, $J = 4.57$ Hz, 2H), 7.74 (d, $J = 6.1$ Hz, 1H), 7.80 (t, $J = 7.6$ Hz, 1H), 11.27 (bs, 1H), 12.17 (bs, 1H); ^{13}C NMR (DMSO- d_6) δ : 188.6, 168.8, 161.5, 158.0, 151.9, 150.4, 143.8, 142.7, 140.7, 136.6, 135.9, 133.4, 127.4,

123.9, 123.9, 122.0, 121.3, 117.7, 116.3, 107.4, 64.8; HRMS m/z (ESI) calcd for $\text{C}_{22}\text{H}_{13}\text{N}_3\text{O}_5 + \text{Na}^+$ 422.0770, found 422.0753.

5-[4-(Trifluoromethoxy)phenyl]-1H-indeno[2',1':5,6]pyrido[2,3-d]pyrimidine-2,4,6(3H)-trione (**24o**). 95%; ^1H NMR (DMSO- d_6) δ : 7.39 (s, 4H), 7.61 (d, $J = 5.8$ Hz, 2H), 7.83 (d, $J = 19.8$, $J = 5.8$ Hz, 2H), 11.35 (s, 1H), 12.27 (s, 1H); ^{13}C NMR (DMSO- d_6) δ : 168.9, 161.7, 158.0, 150.6, 150.4, 148.6, 140.7, 140.1, 136.6, 136.1, 134.1, 133.6, 130.6, 130.4, 124.1, 122.2, 121.1, 120.1, 107.3; HRMS m/z (ESI) calcd for $\text{C}_{21}\text{H}_{10}\text{F}_3\text{N}_3\text{O}_4 + \text{Na}^+$ 448.0521, found 448.0513.

Determination of in Vitro Anticancer Activity. The histological types and the origin of the eight cancer cell lines are detailed in the legend to Table 1. The cells were cultured in MEM (Invitrogen, the U373 cell line) and in RPMI (Invitrogen; the remaining cell lines) media supplemented with 5% heat inactivated fetal calf serum (Invitrogen). All culture media were supplemented with 4 mM glutamine, 100 $\mu\text{g}/\text{mL}$ gentamicin, and penicillin-streptomycin (200 U/mL and 200 $\mu\text{g}/\text{mL}$) (Invitrogen).

The overall growth level of human cancer cell lines was determined using the colorimetric MTT (3-[4,5-dimethylthiazol-2-yl]diphenyl tetrazolium bromide, Sigma) assay.¹⁶ Briefly, the cell lines were incubated for 24 h in 96-well plates (at a concentration of 10,000 to 40,000 cells/mL culture medium depending on the cell type) to ensure adequate plating prior to cell growth determination. The assessment of cell population growth by means of the MTT colorimetric assay is based on the capability of living cells to reduce the yellow product MTT to a blue product, formazan, by a reduction reaction occurring in the mitochondria. The number of living cells after 72 h of culture in the presence (or absence: control) of the various compounds is directly proportional to the intensity of the blue, which is quantitatively measured by spectrophotometry—in our case using a Biorad model 680XR (Biorad, Nazareth, Belgium) at a 570 nm wavelength (with a reference of 630 nm). Each set of experimental conditions was carried out in sextuplicate.

Quantitative Videomicroscopy. The direct visualization of U373 glioblastoma behavior after the treatment with various compounds under study, i.e. inhibition of cell proliferation (a cytostatic effect) versus direct induction of cell death (a cytotoxic effect), was carried out by means of computer-assisted phase contrast microscopy, i.e. quantitative videomicroscopy, as detailed elsewhere.¹⁹

Topoisomerase I Assay. Topoisomerase I activity in the presence of the tested compounds was determined as relaxation of supercoiled pGEM1 plasmid DNA by nucleic extract from MCF-7 cells as described previously.²¹ Briefly, 250 ng of plasmid DNA (pGEM1) was incubated for 30 min at 37 °C with rising concentrations of the test compounds (10–250 μM) in a final volume of 30 μL containing 0.1 μL of nucleic extract, 10 mM Tris (pH 7.9), 100 mM KCl, 10 mM MgCl_2 , 0.5 mM dithiothreitol (DTT), 0.5 mM EDTA, and 0.03 mg/mL bovine serum albumin (BSA). Camptothecin (100 μM) was used as positive control. The reaction was stopped by incubation with 5 μL 5% SDS containing 1 mg/mL proteinase K at 37 °C for 30 min. Subsequently, samples were separated by submarine 1% agarose gel electrophoresis (55 V, 2 h) and gels were stained with 10 $\mu\text{L}/100$ mL ethidium bromide for 20 min. UV-transilluminated gels were documented by Multi-Analyst software.

Topoisomerase II Assay. The effects of **18h,o** and **13h,o** on the catalytic activity of topoisomerase II were determined using a decatination assay. 0.2 μg catenated kinetoplast DNA (KDNA) (TopoGEN, Ohio) was incubated at 37 °C for 1 h in the presence of the test compounds in a final volume of 20 μL containing 50 mM Tris-Cl (pH 8.0), 150 mM NaCl, 10 mM MgCl_2 , 5 mM ATP, 0.5 mM DTT, and 30 $\mu\text{g}/\text{mL}$ BSA. Doxorubicin at 5 μM was used as positive control. The reaction was stopped by further 30 min incubation at 37 °C with 3 μL SDS containing 1 mg/mL proteinase K. Gel electrophoresis and detection were performed as described above. Subsequently, samples were separated by submarine 1% agarose gel electrophoresis (55 V, 2 h) and gels were stained with 10 $\mu\text{L}/100$ mL ethidium bromide for 20 min. UV-transilluminated gels were documented by Multi-Analyst software.

■ ASSOCIATED CONTENT

S Supporting Information. Results of the computer modeling experiments. This material is available free of charge via the Internet at <http://pubs.acs.org>.

■ AUTHOR INFORMATION

Corresponding Author

*Telephone: +1 575 835 5884. Fax: +1 575 835 5364. E-mail: akornien@nmt.edu. Telephone: +1 575 835 6886. Fax: +1 575 835 5364. E-mail: imagedov@nmt.edu.

■ ACKNOWLEDGMENT

This work is supported by the U.S. National Institutes of Health (Grants RR-16480 and CA-135579) under the BRIN/INBRE and AREA programs. J.J.Y. and C.G.B. acknowledge NIH Grant 1U54MH084690. B.L.C. is the holder of a *Grant Télévie* from the *Fonds National de la Recherche Scientifique* (FNRS, Belgium), and R.K. is a Director of Research with the FNRS.

■ ABBREVIATIONS USED

ATCC, American Type Culture Collection; DMEM, Dulbecco's modified Eagle's medium; DMF, dimethylformamide; DMSO, dimethyl sulfoxide; DSMZ, Deutsche Sammlung von Mikroorganismen und Zellkulturen; ECACC, European Collection of Cell Culture; EDTA, diaminethanetetraacetic acid; EtOH, ethanol; FBS, fetal bovine serum; FITC, fluorescein isothiocyanate; FOG, Ficoll Orange G; HEPES, 4-(2-hydroxyethyl)-1-piperazine-thanesulfonic acid; HHB, Heinz-HEPES buffer; HRMS, high resolution mass spectrometry; MCR, multicomponent reaction; MTT, 3-(4,5-dimethylthiazol-2-yl)-2,5-diphenyltetrazolium bromide; SAR, structure-activity relationship; TLC, thin layer chromatography; SD, standard deviation

■ REFERENCES

(1) Newman, D. J.; Cragg, G. M.; Snader, K. M. Natural products as sources of new drugs over the period 1981–2002. *J. Nat. Prod.* **2003**, *66*, 1022–1037.

(2) See for examples: (a) Kissau, L.; Stahl, P.; Mazitschek, R.; Giannis, A.; Waldmann, H. Development of Natural Product-Derived Receptor Tyrosine Kinase Inhibitors Based on Conservation of Protein Domain Fold. *J. Med. Chem.* **2003**, *46*, 2917–2931. (b) Boldi, A. M. Libraries from natural product-like scaffolds. *Curr. Opin. Chem. Biol.* **2004**, *8*, 281–286.

(3) For utilization of MCR in drug discovery, see: Hulme, C.; Gore, V. Multi-component reactions: Emerging chemistry in drug discovery. From xylocaïn to crivivan. *Curr. Med. Chem.* **2003**, *10*, 51–80.

(4) (a) Magedov, I. V.; Manpadi, M.; Rozhkova, E.; Przheval'skii, N. M.; Rogelj, S.; Shors, S. T.; Steelant, W. F. A.; Van slambrouck, S.; Kornienko, A. Structural simplification of bioactive natural products with multicomponent synthesis: Dihydropyridopyrazole analogues of podophyllotoxin. *Bioorg. Med. Chem. Lett.* **2007**, *17*, 1381–1385. (b) Magedov, I. V.; Manpadi, M.; Van Slambrouck, S.; Steelant, W. F. A.; Rozhkova, E.; Przheval'skii, N. M.; Rogelj, S.; Kornienko, A. Discovery and Investigation of Antiproliferative and Apoptosis-Inducing Properties of New Heterocyclic Podophyllotoxin Analogues Accessible by a One-Step Multicomponent Synthesis. *J. Med. Chem.* **2007**, *50*, 5183–5192. (c) Magedov, I. V.; Manpadi, M.; Evdokimov, N. M.; Elias, E. M.; Rozhkova, E.; Ogasawara, M. A.; Bettale, J. D.; Przheval'skii, N. M.; Rogelj, S.; Kornienko, A. Antiproliferative and apoptosis inducing properties of pyrano[3,2-c]pyridones accessible by a one-step multicomponent synthesis. *Bioorg. Med. Chem. Lett.* **2007**, *17*, 3872–3876.

(d) Magedov, I. V.; Manpadi, M.; Ogasawara, M. A.; Dhawan, A. S.; Rogelj, S.; Van slambrouck, S.; Steelant, W. F. A.; Evdokimov, N. M.; Uglinski, P. Y.; Elias, E. M.; Knee, E. J.; Tongwa, P.; Antipin, M. Y.; Kornienko, A. Structural Simplification of Bioactive Natural Products with Multicomponent Synthesis. 2. Antiproliferative and Antitubulin Activities of Pyrano[3,2-c]pyridones and Pyrano[3,2-c]quinolones. *J. Med. Chem.* **2008**, *51*, 2561–2570.

(5) Lorence, A.; Nessler, C. L. Molecules of interest—Camptothecin, over four decades of surprising findings. *Phytochemistry* **2004**, *65*, 2735–2749.

(6) Pizzolato, J. F.; Saltz, L. B. The camptothecins. *Lancet* **2003**, *361*, 2235–2242.

(7) Driver, R. W.; Yang, L. X. Synthesis and pharmacology of new camptothecin drugs. *Mini-Rev. Med. Chem.* **2005**, *5*, 425–439.

(8) Thomas, C. J.; Rahier, N. J.; Hecht, S. M. Camptothecin: current perspectives. *Bioorg. Med. Chem.* **2004**, *12*, 1585–1604.

(9) Dallavalle, S.; Ferrari, A.; Biasotti, B.; Merlini, L.; Penco, S.; Gallo, G.; Marzi, M.; Tinti, M. O.; Martinelli, R.; Pisano, C.; Carminati, P.; Carenni, N.; Beretta, G.; Perego, P.; De Cesare, M.; Pratesi, G.; Zunino, F. Novel 7-oxyiminomethyl derivatives of camptothecin with potent in vitro and in vivo antitumor activity. *J. Med. Chem.* **2001**, *44*, 3264–3274.

(10) Bom, D.; Curran, D. P.; Kruszewski, S.; Zimmer, S. G.; Strode, J. T.; Kohlhagen, G.; Du, W.; Chavan, A. J.; Fraley, K. A.; Bingchang, A. L.; Latus, L. J.; Pommier, Y.; Burke, T. G. The novel silatecan 7-tert-butyl-dimethylsilyl-10-hydroxycamptothecin displays high lipophilicity, improved human blood stability, and potent anticancer activity. *J. Med. Chem.* **2000**, *43*, 3970–3980.

(11) Lansiaux, A.; Leonce, S.; Kraus-Berthier, L.; Bal-Mahieu, C.; Mazinghien, R.; Didier, S.; David-Cordonnier, M. H.; Hautefaye, P.; Lavielle, G.; Bailly, C.; Hickman, J. A.; Pierre, A. Novel stable camptothecin derivatives replacing the E-ring lactone by a ketone function are potent inhibitors of topoisomerase I and promising antitumor drugs. *Mol. Pharmacol.* **2007**, *72*, 311–319.

(12) Cagir, A.; Jones, S. H.; Gao, R.; Eisenhauer, B. M.; Hecht, S. M.; Luotonen, A. A naturally occurring human DNA topoisomerase I poison. *J. Am. Chem. Soc.* **2003**, *125*, 13628–13629.

(13) Rao, V. A.; Agama, K.; Holbeck, S.; Pommier, Y. Batracylin (NSC 320846), a dual inhibitor of DNA Topoisomerases I and II induces histone gamma-H2AX as a biomarker of DNA damage. *Cancer Res.* **2007**, *67*, 9971–9979.

(14) (a) Deady, L. W.; Desneves, J.; Kaye, A. J.; Thompson, M.; Finlay, G. J.; Baguley, B. C.; Denny, W. A. Ring-substituted 11-oxo-11H-indeno[1,2-b]quinoline-6-carboxamides with similar patterns of cytotoxicity to the dual topo I/II inhibitor DACA. *Bioorg. Med. Chem.* **1999**, *7*, 2801–2809. (b) Deady, L. W.; Kaye, A. J.; Finlay, G. J.; Baguley, B. C.; Denny, W. A. Synthesis and antitumor properties of N-[2-(dimethylamino)ethyl]carboxamide derivatives of fused tetracyclic quinolines and quinoxalines: A new class of putative topoisomerase inhibitors. *J. Med. Chem.* **1997**, *40*, 2040–2046. (c) Catoen-Chackal, S.; Facompre, M.; Houssin, R.; Pommery, N.; Goossens, J. F.; Colson, P.; Bailly, C.; Henichart, J. P. DNA binding to guide the development of tetrahydroindeno[1,2-b]pyrido[4,3,2-de]quinoline derivatives as cytotoxic agents. *J. Med. Chem.* **2004**, *47*, 3665–3673. (d) Malecki, N.; Carato, P.; Rigo, B.; Goossens, J. F.; Houssin, R.; Bailly, C.; Henichart, J. P. Synthesis of condensed quinolines and quinazolines as DNA ligands. *Bioorg. Med. Chem.* **2004**, *12*, 641–647.

(15) Manpadi, M.; Uglinski, P. Y.; Rastogi, S. K.; Cotter, K. M.; Wong, Y.-S. C.; Anderson, L. A.; Ortega, A. J.; Van slambrouck, S.; Steelant, W. F. A.; Rogelj, S.; Tongwa, P.; Antipin, M. Y.; Magedov, I. V.; Kornienko, A. Three-component synthesis and anticancer evaluation of polycyclic indenopyridines lead to the discovery of a novel indenoheterocycle with potent apoptosis inducing properties. *Org. Biomol. Chem.* **2007**, *5*, 3865–3872.

(16) (a) Hayot, C.; Farinelle, S.; De Decker, R.; Decaestecker, C.; Darro, F.; Kiss, R.; Van Damme, M. In vitro pharmacological characterizations of the anti-angiogenic and anti-tumor cell migration properties mediated by microtubule-affecting drugs, with special emphasis on the

organization of the actin cytoskeleton. *Int. J. Oncol.* **2002**, *21*, 417–425. (b) Lamoral-Theys, D.; Andolfi, A.; Van Goietsenoven, G.; Cimmino, A.; Le Calvé, B.; Wauthoz, N.; Mégalizzi, V.; Gras, T.; Bruyère, C.; Dubois, J.; Mathieu, V.; Kornienko, A.; Kiss, R.; Evidente, A. Lycorine, the main phenanthridine Amaryllidaceae alkaloid, exhibits significant antitumor activity in cancer cells that display resistance to proapoptotic stimuli: An investigation of structure-activity relationship and mechanistic insight. *J. Med. Chem.* **2009**, *52*, 6244–6256.

(17) Loza-Mejia, M. A.; Olvera-Vazquez, S.; Maldonado-Hernandez, K.; Guadarrama-Salgado, T.; Gonzalez-Sanchez, I.; Rodriguez-Hernandez, F.; Solano, J. D.; Rodriguez-Sotres, R.; Lira-Rocha, A. Synthesis, cytotoxic activity, DNA topoisomerase-II inhibition, molecular modeling and structure-activity relationship of 9-anilinothiazolo[5,4-b]quinoline derivatives. *Bioorg. Med. Chem.* **2009**, *17*, 3266–3277.

(18) (a) Lefranc, F.; Mijatovic, T.; Kondo, Y.; Sauvage, S.; Roland, I.; Krstic, D.; Vasic, V.; Gailly, P.; Kondo, S.; Blanco, G.; Kiss, R. Targeting the alpha-1 subunit of the sodium pump (the Na⁺/K⁺-ATPase) to combat glioblastoma cells. *Neurosurgery* **2008**, *62*, 211–222. (b) Ingrassia, L.; Lefranc, F.; Dewelle, J.; Pottier, L.; Mathieu, V.; Spiegl-Kreinecker, S.; Sauvage, S.; El Yazidi, M.; Dehoux, M.; Berger, W.; Van Quaquebeke, E.; Kiss, R. Structure-activity-relationship analysis of novel derivatives of narciclasine (an Amaryllidaceae Isocarboxystyryl alkaloid) as potential anti-cancer agents. *J. Med. Chem.* **2009**, *52*, 1100–1114.

(19) (a) De Hauwer, C.; Camby, I.; Darro, F.; Migeotte, I.; Decaestecker, C.; Verbeek, C.; Danguy, A.; Brotchi, J.; Salmon, I.; Van Ham, Ph.; Kiss, R. Gastrin inhibits motility, decreases cell death and increases cell proliferation in human glioblastoma cell lines. *J. Neurobiol.* **1998**, *37*, 373–382. (b) Lamoral-Theys, D.; Pottier, L.; Kerff, F.; Dufrasne, F.; Proutière, F.; Wauthoz, N.; Neven, P.; Ingrassia, L.; Van Antwerpen, P.; Lefranc, F.; Gelbcke, M.; Pirotte, B.; Kraus, J. L.; Nève, J.; Kornienko, A.; Kiss, R.; Dubois, J. Simple di- and trivanillates exhibit cytostatic properties toward cancer cells resistant to pro-apoptotic stimuli. *Bioorg. Med. Chem.* **2010**, *18*, 3823–3833.

(20) Habermeyer, M.; Fritz, J.; Barthelmes, H. U.; Christensen, M. O.; Larsen, M. K.; Boege, F.; Marco, D. Anthocyanidins modulate the activity of human DNA topoisomerases I and II and affect cellular DNA integrity. *Chem. Res. Toxicol.* **2005**, *18*, 1395–1404.

(21) Dormetshuber, R.; Heffeter, P.; Lemmens-Gruber, R.; Elbling, L.; Marko, D.; Micksche, M.; Berger, W. Oxidative stress and DNA interactions are not involved in Enniatin- and Beauvericin-mediated apoptosis induction. *Mol. Nutr. Food Res.* **2009**, *53*, 1112–1122.